

MEASURING THE KINETIC ENERGY DISSIPATION EFFECTS OF ROCK FALL ATTENUATING SYSTEMS WITH VIDEO ANALYSIS

James Glover¹, Matthias Denk², Franck Bourrier³, Axel Volkwein⁴ and Werner Gerber⁴

ABSTRACT

Attenuation is the reduction in intensity of any flux through a medium. Rock fall attenuator systems are structures made of flexible wire netting designed to reduce the intensity (kinetic energy) of rock fall and guide their trajectory. In order to evaluate the protective effect of an attenuating system and their capacity to absorb high energy impacts, high speed video recording methods have been applied to capture full scale rock rolling and attenuator barrier tests. The application of video methods requires that individual frames are scaled to the plane of the rock fall. Following this the rock fall trajectory and velocity over time can be extracted from the video. Herein, an assessment of the error in different approaches to video image scaling and position tracking for video analysis is made. Additionally the trajectories and velocity of rock falls from both un-attenuated rock rolling experiments and experiments testing the rock fall attenuator systems are analysed. A comparison of these data has allowed an assessment of the energy absorbed by the attenuator systems. Additionally, restitution coefficients for impacts on hard rock slopes have been drawn from the data, assisting in a simple model applied to estimate the attenuation effects of rock fall attenuator systems.

Keywords: Rock fall; flexible netting; attenuator systems; design; video tracking

INTRODUCTION

Rock fall attenuator systems are designed with the aim of intercepting rock fall trajectory, guiding it under a tail drape and dampening bounce heights (Figs. 1). This offers the potential to dissipate large portions of the kinetic energy through barrier impacts deforming the netting and interaction with the slope during its transport to the base of slope (Badger et al., 2008). Application of rock fall attenuator systems are suited to regions of high frequency rock fall whereby cleaning and maintenance can be better managed as opposed to standard rock fall barriers that catch and contain rock fall. Or for situations where existing protection measures, such as rock fall galleries, do not meet the required energy level of rock fall hazard. Attenuator systems can be applied to dissipate the energy of rock fall to the design value of the existing installations or site specific design conditions.

It has become apparent that much of the energy dissipation capacity of these systems can be attributed to ground impacts, and the ability of the netting to redirect the rock boulder to ground contact. This highlights how these systems should be considered in combination with the underlying terrain as well as the expected rock fall hazard.

Given their intended design function, an evaluation of their ability to reduce rock fall velocity, bounce heights, and respectively its energy, is required. Without such data the attenuating effect would not be quantifiable and hence a good data evaluation has highest priority. In order to measure these effects, information of the position and accelerations of the boulders must be gathered from experiments with attenuator systems and free rolling rock tests. The use of natural rock boulders in these experiments dictated that video analysis must be used to capture the relevant data. This was chosen over and above growing capabilities of internal measurement techniques. In this contribution we therefore concentrate on a description of the video capture and analysis techniques, assessing their practicality and quality.

¹ WSL Institute for Snow and Avalanche Research, Flüelastr. 11, 7260 Davos, Switzerland
(e-mail: james.glover@wsl.ch)

² Geobruigg AG, Romanshorn, Switzerland

³ CEMAGREF, Grenoble, France

⁴ Swiss Fed. Research Institute WSL, Birmensdorf, Switzerland

Illustrating possible errors along with tools to test error, and provide an example result set applying it to the problem of quantifying the attenuation effect of rock fall attenuator systems.



Figs. 1 Catchment area of attenuating structure (left) and guided boulder along rock face (right)

EXPERIMENTAL SETUP

At a quarry in St Léonard (Switzerland) a rock fall launching facility has been constructed. It consists of a ramp constructed of an inclined net held up by an old crane. A release mechanism designed to contain natural rock boulders is hoisted up onto the launch ramp with the use of a mobile crane. The net ramp guides the boulders down the ramp which ends at the edge of a 50 m long, 50 ° steep limestone rock slope (Fig. 2 left). Rock boulders used for the experimentation were natural rocks sourced from the local quarry. They ranged from 500 kg – 2000 kg, and were composed of either limestone or quartzite. Steel posts placed at the edge of the slope facilitated full scale rock fall netting to be mounted and rock fall attenuator barrier designs to be tested. The run out area at the bottom of the slope is short and is protected with a low deflection rock fall barrier (Fig. 2 right) and large earth dams, these safety measures not only ensure safe testing of the attenuator systems but have also enabled rock rolling experiments without the presence of the attenuator nets. The ability to carry out comparative tests is the key to being able to assess the working attenuation effect the attenuator systems have on the passage of rock fall. Moreover, rock rolling experiments without the influence of netting (Fig. 2 right) provide important data for the calibration of rock fall modelling codes.

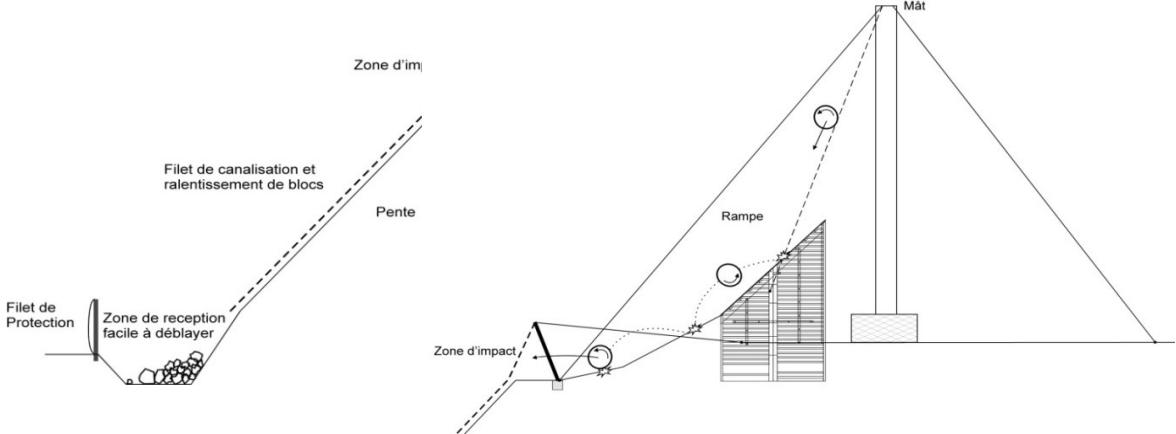
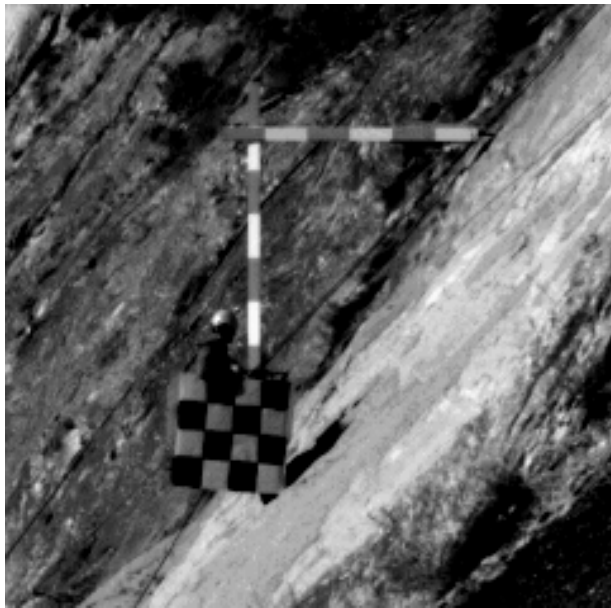


Fig. 2 Sketch of acceleration ramp (right) and hillslope for (un-)attenuated rock falls (left)

The chosen data capture method was video. In addition for the tests with attenuator netting load cells mounted in the support ropes measured the tensional load they incurred. The video method applied in all tests has been adapted from the standardised procedure for testing rock fall barriers (Gerber, 2001). The video cameras are positioned to obtain as near as possible an orthogonal perspective to the plane of the rock fall trajectory capturing its horizontal and vertical position over time. Strong deviations from this situation induce anisotropies in the image scaling which can be problematic for the video analysis phase. Video cameras used were capable of between 30 and 1000 fps. For trajectory plotting

50 fps is sufficient, while detailed imaging of the impact phase 250 fps was selected for the cameras with this capability. In all, eight video cameras were installed along the profile of the slope allowing the capture of the full rock fall trajectory with sufficient detail for the video analysis. Particular areas of interest for the tests with rock fall netting were the zone of initial interception and the exit from the barrier. An additional video camera placed with a front view of the rock slope parallel with the plane of the rock fall facilitated the capture of the lateral deviations of the rock boulders from the fall line of the slope. This also assisted in measuring the depth of the rock boulder in the images of the cameras placed along the slope profile. This is important for the scaling of the video images.

Scaling of the video images was achieved by placing targets or scale bars in the video image with known dimensions (Fig. 3). These can be temporarily placed in the camera view prior to testing or can be fixed as permanent features, both methods were applied during the experiments. The former solution requires that images of the temporary targets are taken with the cameras used for the experiments and dictates that these camera settings (zoom, aspect) cannot be altered during testing.



The scale bars allow the pixels in the raster of the video images to be scaled to the plane of the rock fall trajectory. To achieve this, the distance between the scale bar and the camera in addition to the flight path of the rock fall and the camera must be known. Two methods were trailed to achieve this. The first was a direct measurement of positions of the cameras and the scale bars using the Leica 1200 differential GPS and total station. Where possible the impact points of the rock boulders were measured using the theodolite, this was achieved by looking back over video footage after each rock fall event. The second only used the images captured with the front view camera, working only in a pixel scale to calculate the relative distance of impact points from the known scale bars locations and the cameras.

Fig. 3 Permanent scale bars fixed at the far edge of the test slope 46.7 m from the camera, the spacing of stripes are 50 cm. The temporary target for scaling the video is held in the centre of the slope at 36.3 m from the camera, the squares are 25 x 25 cm. This image highlights the scale change with the depth in the picture

ANALYSIS METHODS

The video analysis was performed using two similar methods of boulder position tracking. The first utilised an image tracking software WINalyze (Mikromak, 2010). The second was an algorithm written for a Matlab environment. Each method requires scaling of the image raster in every frame of the video captured. For the scaling, four different approaches were tested and allowed an assessment of any potential scaling errors introduced to the footage through the video set up and applied methodology. The four methods were as follows:

- a) Image raster is scaled to the distant fixed scale bar then recalibrated to the plane of the passing rock boulder by taking the measured position of the nearest impact as the distance to the camera. The distance between the camera, scale bar, and passing boulder are surveyed with a Leica 1200 total station.
- b) The image raster was scaled using the four nearest targets from the trajectory to be analysed. These targets were identified using the frontal video. The average of the scaling factors associated with these targets was finally taken as scaling factor.

- c) The image raster was scaled using the four nearest targets from the trajectory to be analyzed. These targets were identified using the frontal video. The scaling factor for one trajectory was calculated by balancing the mean scaling factors associated with the two nearest and the two farthest targets in relation to their mean distance to the analyzed trajectory. All these distances were measured using the front view camera only.
- d) The image raster was scaled using the four nearest targets from the trajectory to be analyzed. These targets were identified using the frontal video. The scaling factor was calculated for each measurement point of the analyzed trajectory. The scaling factor associated with each measurement point is calculated by balancing the mean scaling factors associated with the two nearest and with the two farthest targets using the distance from the measurement point to the two nearest and to the two farthest targets. All these distances were measured using the front view camera only.

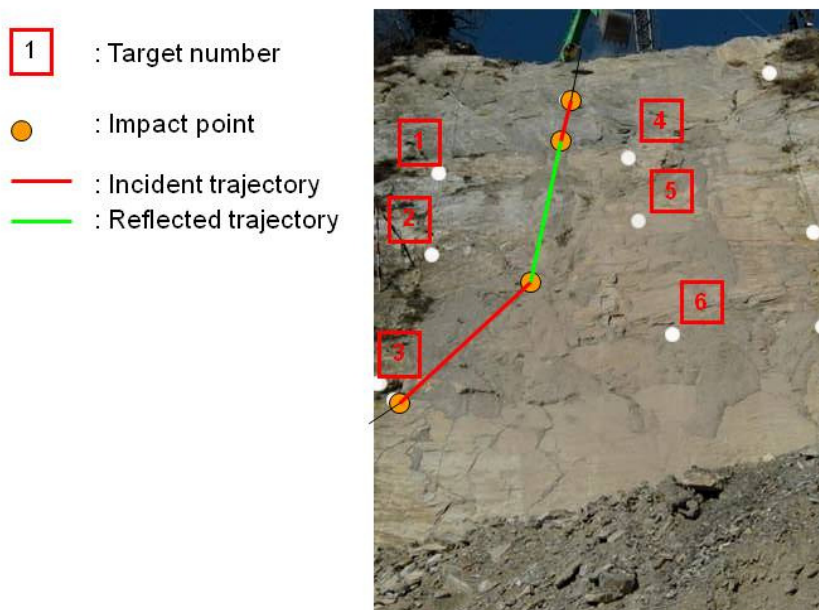


Fig. 4 Front view camera with temporary targets and impact points from example rock fall experiment

Both programs plot the position of the rock boulder in the coordinate system of the 2D image raster set by the scaling procedure. The WINanalyze video analysis software (Mikromak, 2010) has an image tracking algorithm which permits some automation of position plotting. It seeks changes in the image about a user defined searching window and plots the centre of mass of the rock boulder. This function requires a reasonably high degree of contrast between the moving object and the background of the image. With a poor contrast the image tracking algorithm has difficulty finding the centre of mass of the passing rock boulder. This was often found to be the case for testing, particularly when using natural rock boulders, and for images that were over exposed due to the situation of the cameras and the position of the sun. In this case it is possible to manually position the search window over the rock boulders centre of mass.

A second position detection program was developed under Matlab environment. Three different detection methods were applied. First, an automatic approach based on image correlation was built. In this first method, an initial shape is defined in the first image and the location and the orientation of this shape is detected in the following image by correlation analysis. This method was not used in the following since, as for the Winanalyze tracking algorithm, the quality of the images was not sufficient for various reasons. For example, the rotation of the boulder out of the camera frame and the additional objects in the image such as smaller rocks and dust made the correct detection of the boulder shape from one image to the following difficult to match. Finally, the two other manual gravity centre detection methods were used. These two methods consisted of either clicking around the whole object to be followed in the image, the algorithm automatically calculating its gravity centre and

orientation. Or by clicking directly the “estimated” gravity centre of the object and counting the number of images for the rock to make a complete (or half) rotation.

Once the position data of the rock boulder in the horizontal (x) and vertical (z) plane is captured, from the video footage for each frame, it can be used to perform the trajectory analysis and a calculation of the instantaneous translational velocity of each component of its trajectory. A final check of the potential error in the scaling of the image is performed by assessing the values generated from a regression analysis of the vertical (z) positions over time, and comparing this to the acceleration expected due to gravity since this is the only acceleration expected in this axis. If the scaling is correct then the values generated for the vertical axis should fit the expected parabola of an object in free fall due to gravity.

OBTAINED RESULTS

In all, 15 rock rolling experiments without the presence of an attenuator system were performed, this amounted to over 30 slope impacts. The average number of impacts during an experiment was two. These experiments were complimented by over 40 tests involving the rock fall attenuator system conducted prior to the rock rolling exercise. In the following section we explore the methodologies applied to capture the boulder position by using test five from the rock rolling experiments to compare between methods.

Plotting the (x z) position of boulder trajectories reveals a reasonably smooth fit to an expected parabola, the calculated parabola for each portion of the trajectory are laid on top of the raw data (Fig. 5). While a differentiation of these positions over time to calculate the instantaneous velocity of the rock boulder reveals strong level of noise in the data (Fig. 6). This is of course a result of the

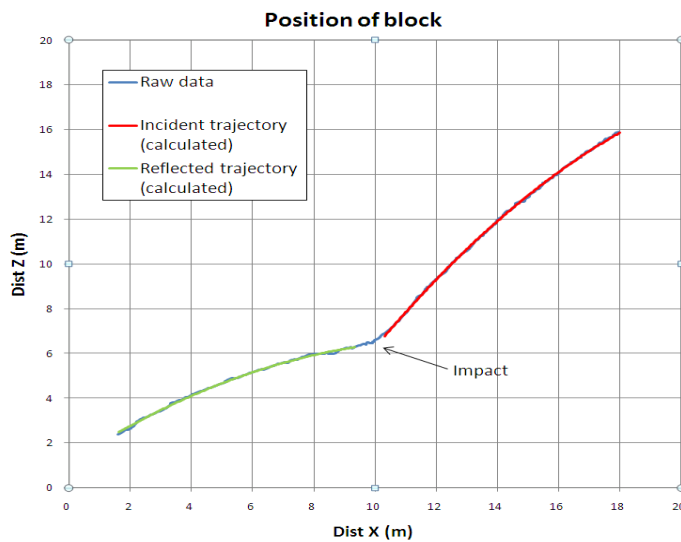


Fig. 5 Trajectory of rock boulder from example test

amplification of small positional errors incurred during the tracking of the boulder position due to the use of a finer time step resolution from the higher frame rate video. To assess the error, a running standard deviation was applied over three instantaneous positions and the velocity. For the position of the centre of mass standard deviation was between +/- 0.7 and +/- 0.9 cm for the vertical and horizontal axes over the tests. While for the velocities this relatively small and acceptable error in position translates to a standard deviation of between +/- 3.0 and +/- 4.2 m/s . To approach this issue a regression analysis for each the horizontal and the vertical components of the parabola is performed (Fig. 6).

The final velocity is resolved by using the resultant regression analysis to reconstruct the parabola.

Given the assumption that during free flight the rock boulder will only be influenced by gravity the horizontal and vertical components of its parabola can be written separately. Using the vertical trajectory over time and setting a polynomial trend line to the data, the equation of this curve can be compared to that expected for gravity and an assessment of the scaling error can be made.

$$y(t) = \frac{1}{2}gt^2 + bt + c \quad (1)$$

Where g is acceleration due to gravity, t is time, b the initial velocity in the vertical plane and c the start position of the rock boulder. The value of half gravity is used to estimate the error. This error calculated for each scaling method from the vertical component of both the incident and reflected trajectory are plotted in Table 1. Positive values indicate that the scaling results in an underestimation of the boulder velocity while negative values overestimate the boulder velocity.

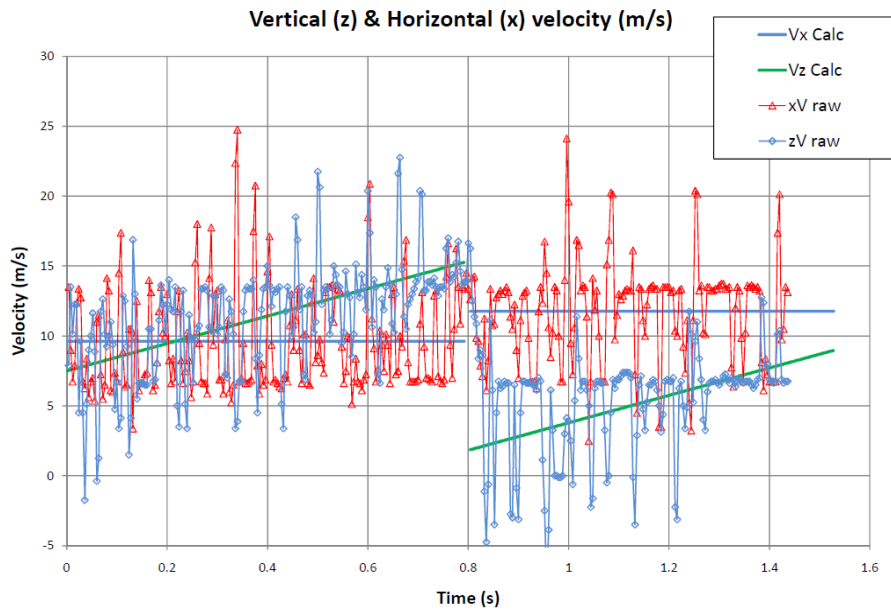
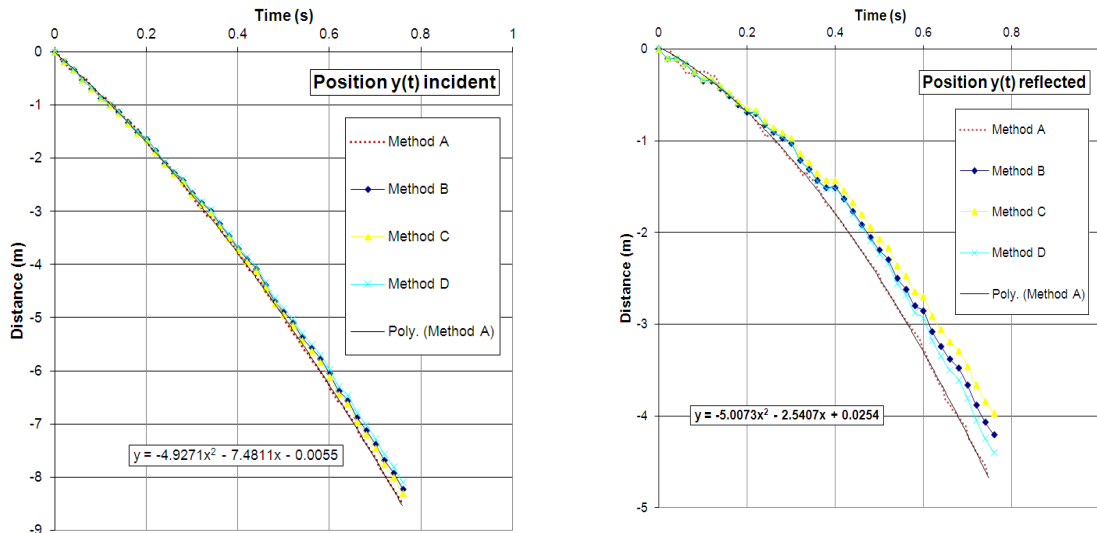


Fig. 6 Instantaneous velocity for horizontal (red) and vertical (blue) components of trajectory with additional regression trend

Tab. 1: Comparison of results using different video analysis methods

Method	A	B	C	D
Absolute velocity incident (m/s)	18.08	17.04	17.18	16.83
Absolute velocity reflected (ms^{-1})	12.04	11.03	10.39	11.43
% error in scaling incident	0.9	7.6	6.7	11.3
% error in scaling reflected	-2.1	8.3	13.4	-4.4
Restitution coefficient				
Normal (R/I)	2.10	2.13	2.07	2.28
Tangential (R/I)	0.59	0.56	0.52	0.59
Absolute (R/I)	0.65	0.65	0.60	0.68

Method A using direct measurements of the scale bar and boulder position using the total station performed the best, with acceptable error in the positioning. It is noted that the scaling set for this method causes acceleration in the reflected trajectory. This is expected since method A assumes that the boulder passes through the video image in an oblique plane, it does not allow for deviation of the boulder from the scaled plane. Given that after the impact recorded for test five captures the boulder deviating to the left of the fall line as viewed from the frontal video camera (Fig. 4), this causes a distance increase between the camera and the boulder and respectively acceleration due to the error in the scaling. For methods B, C, and D, the error due to scaling increases. One of the main reasons for this is the use of the frontal video camera to perform the recalibration of the scaling to the plane of the rock boulder. Since this method relies on measurements from an additional image sequence it can also be necessary to scale these images. In this case the image was assumed to be constant and no scaling was applied. However, with a horizontal camera view onto the 50° rock slope it is evident that this has introduced anisotropies into the image scaling from the top to the bottom of the image. This effect is most evident in method D where an instantaneous scaling of the images was applied to account for the lateral position of the boulder captured with the front view camera. For the incident trajectory it strongly underestimates the position of the boulder setting it too close to the camera resulting in slower velocity. While for the reflected trajectory it then overestimates the position. This is to be expected when looking at the image from the frontal view, due to the view angle of this camera, the upper portion of this video has a much wider field of view than the bottom (Fig. 4).

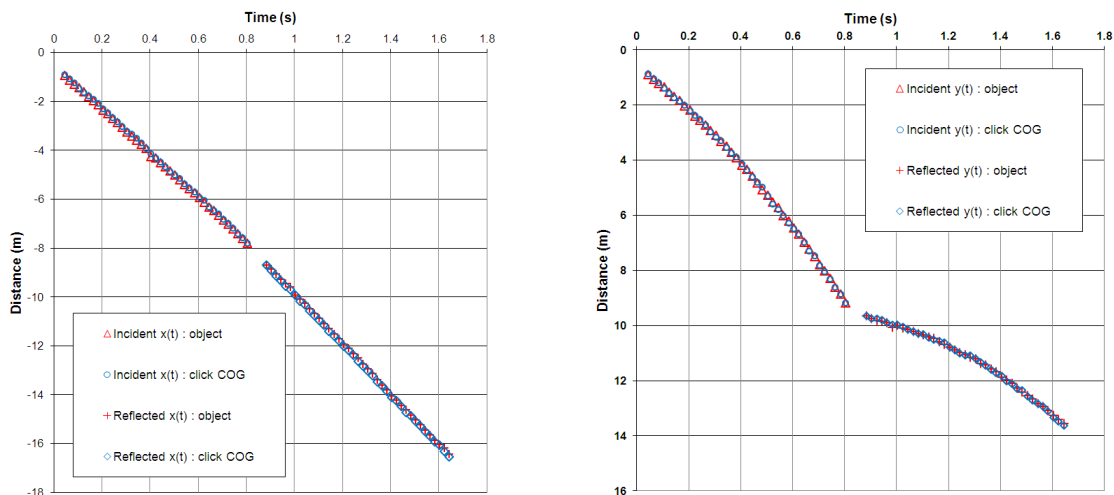


Figs. 7 Comparison of position plotting for scaling methods A, B, C, and D. (left) vertical positions over time for incident trajectory, the trend curve and equation is plotted for method A illustrating its similarity to that expected from equation (1), (right) reflected trajectory

Using the Matlab position tracking algorithm, the resultant differences in trajectory positioning were assessed due to the respective position plotting methods. The two methods assessed were a manual selection of the centre of gravity, and centre of gravity calculated from manually selected points delineating the edge of the object. The results from this comparison are displayed in Figures 8, and reveal no significant differences between the methods.

APPLICATION TO ATTENUATING EFFECT

Prior to the un-attenuated rock rolling experiments six test series involving impacts with an attenuator system were conducted, this generated a data bank of over 40 individual tests. The primary data collected was the initial impact velocity of the rock boulder into the netting, its exit velocity from the netting, and the force incurred by the system ropes. Using the previously described video capture and analysis techniques this has provided a data set to assess the attenuation affect of the rock fall attenuator system in comparison to the velocities of the rock boulders that where rolled un-attenuated.



Figs. 8 Comparison of manual centre of gravity picking and calculated from points around object manually selected. (left) Horizontal position x over time, and (right) vertical position y over time

In an attempt to quantify the attenuation effects of the attenuator systems, two experiments have been selected for comparison from both the attenuated and un-attenuated testing series. The comparative data sets have been selected such that the total potential energy from the rock release point to its containment in the low deflection barrier was more or less the same. This is the same mass of the rock

boulder and same release height. In this simple comparison the velocity and respectively the kinetic energy attained by the rock boulder during the un-attenuated experiments is assumed as a bench mark from which to assess the rock fall attenuator netting system. The kinetic energy is calculated over the velocity the rock boulder attains at the point the rock boulder leaves the rock fall attenuator system before contacting the low deflection barrier. The attenuation capacity is calculated by dividing the exit kinetic energy of the attenuated experiment by the kinetic energy of the equivalent un-attenuated experiment. The results of the comparison are presented in Table 2.

Tab. 2: Comparison between un-attenuated and attenuated rock fall events

Test	Un-attenuated	Attenuated	Un-attenuated	Attenuated
	(A)	(A)	(B)	(B)
Mass (kg)	1130	1190	820	870
Height potential (m)	45	50	35	35
V_{exit} (ms ⁻¹) – measured	22.7	15.7	18.3	9.6
E_{exit} (kJ) – measured	292	147	138	40
System attenuation	-	50%	-	71%

The comparisons suggest that the presence of the rock fall attenuator system can attenuate between 50 and 71 % of the kinetic energy that would otherwise arrive at the base of the slope if the rock boulder is allowed to roll un-attenuated.



Figs. 9 (left) low deflection barrier with rock fall attenuator protection (20 attenuated impacts), (right) low deflection barrier after 8 un-attenuated impacts during the rock rolling experiments

Qualitatively the effects of the rock fall attenuator system also are very apparent. Figures 9 illustrate the same low deflection barrier that was used in addition to large earth dams as part of the safety measures during testing of the rock fall attenuators and for rock rolling experiments without an attenuator system. The low deflection barrier served its intended purpose of collecting rock boulders exiting from the attenuator system. During the testing series with the presence of an upslope attenuator system it retained over 20 rock boulders, it did so without significant damages that would warrant repair maintaining its functional capacity throughout. While for the experiments without the use of the rock fall attenuator system (Fig. 9 right), the potential damages of an un-attenuated rock fall for this given test slope are clearly illustrated. Of the 15 experiments during the rock rolling experiments, the low deflection barrier received 8 un-attenuated rock fall impacts with energies at or over the design limit of the barrier. The remaining 7 of the 15 had bounce heights that exceeded the barrier design height; this was anticipated for the un-attenuated experiments and they were safely contained by the earth dam. Although structural damages of the low deflection barrier system were incurred, of all rock falls that landed in the system all were retained and stopped within a maximum deflection distance of 1.5 m, in this respects the low deflection barrier functioned entirely as intended. Due to the low deflection function of this system the intended design is that system parts such as ropes and post that

received direct impacts are replaced after individual rock fall events. Not least after the multiple impacts that it was subject to in this case.

This example clearly illustrates the attenuating capabilities of rock fall attenuator systems, and demonstrates how attenuator systems can be applied to dissipate the energy of rock fall to the design value of the existing installations or site specific design conditions.

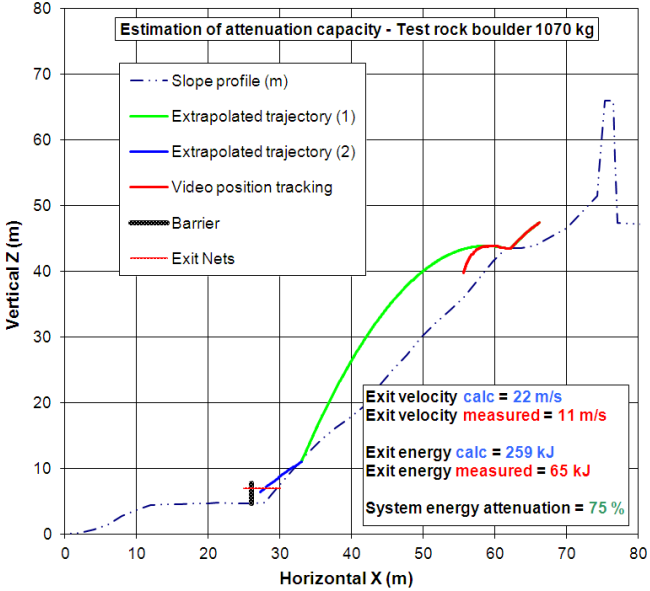
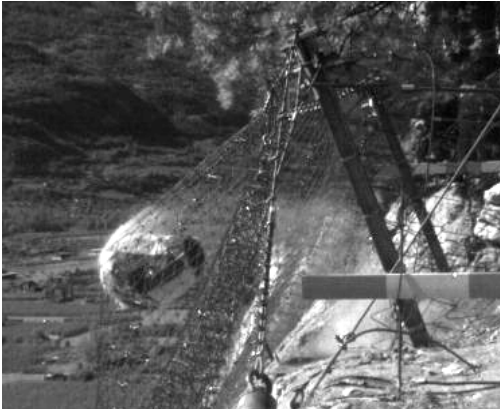


Fig. 10 High speed video image of first impact into attenuator system (left); measured and extrapolated trajectory with and without attenuating system (right)

It is not always practical to conduct rock rolling experiments, and in an attempt to further assess the attenuation capacity of the attenuated experiments a simple 2D model has been constructed (Fig. 10). Figures 10 illustrate the redirection of an impacting rock boulder when it is caught by the rock fall attenuator system. The figure to the right plots the actual trajectory of the rock boulder during the experiment. Using the previously described regression technique, sampling the flight path prior to contact with the nets, a theoretical trajectory (without the influence of the attenuator netting) can be extrapolated. This is taken to the point of contact with the known slope topography and a restitution coefficient is applied to model the respective velocity and energy lost during this contact. The trajectory is then extrapolated further. Reading of the modelled velocity at the same point the boulder would normally exit the rock fall attenuator system. In this case the results of the rock rolling experiments have allowed an estimation of this restitution coefficient for this given test slope and was applied to this model. The modelled exit velocity was 22 ms^{-1} which for this particular example results in an estimated 75% system energy attenuation.

CONCLUSIONS

The application of video analysis techniques capturing rock fall velocity for free and attenuated rock falls has enabled an assessment of the attenuation effect of rock fall attenuator systems. An understanding of the design controls available to optimizing the dissipation effects of the netting is crucial to their application. With quantitative information of the kinetic energy dissipation effects of rock fall attenuator systems, installed attenuators can be better designed to site specific rock fall problems and design goals. Important for their design is to consider how these systems work in conjunction with the terrain in which they are installed. Choice of netting properties (weight, length and mesh size) that are tailored to terrain properties (slope angle, surface roughness, and material), and expected rock fall hazard (shape, size, and velocity), are the challenging decisions the rock fall engineer must face. With the experiences from full scale testing, we are coming closer to design guides that will be able to direct such design decisions.

Trials with different scaling methodologies have highlighted various errors possible. It has shown that a direct measure of the scaling target and nearest impact zone is the most accurate. While if a constant plane is assumed it doesn't account for the lateral deviations of the rock boulder from the fall line consequently adding error into the analysis. Thus a combination of scaling methods A and D are considered to give the best results. For a future application of this method, the frontal video must also be scaled, especially when an orthogonal perspective is not possible due to the given slope angle. Taking the data for the vertical component of the plotted trajectory over time and comparing the polynomial trend to that expected for gravity has proved a useful tool in assessing any potential error in scaling any video images (Figs. 7).

The tracking techniques applied to plot the position of the rock boulder centre of gravity showed little variation in the resultant data, all generating positional data with minimal error that is acceptable for trajectory analysis. However, when calculating instantaneous velocities an amplification of this error becomes unacceptable, generated through an increase in the frame rate selected. To approach this a regression analysis of the data is used to reconstruct the trajectory and respectively the velocity.

The experimentation has permitted the estimation of normal and tangential coefficients of restitution for hard rock impacts on solid limestone rock slope. For the relatively steep test slope between 40 and 55 ° we calculate normal and tangential restitution coefficients of around 2.0 and 0.6 respectively. This has been useful in assisting a simplified model to assess the attenuation effects of the rock fall attenuators. Moreover, these data will prove useful for the calibration of sophisticated 3D numerical rock fall codes (RAMMS, 2010; Rockyfor3D, 2010). It should be noted that the values for the normal restitution coefficient is greater than 1. Thus, for users of lumped mass rock fall models special attention should be paid since this value alone is not sufficient to calibrate such models.

ACKNOWLEDGEMENTS

The Authors wish to thank members of MTA Carrière St Léonard for the use of the test site and excellent assistance during experimentation. Further thanks are to the Commission of Technology and Innovation (CTI) of the Swiss Federal Office for Professional Education and Technology (OPET) who partly fund this project [KTI-Project Nr. 10044.1].

REFERENCES

- Badger, T.C. et al. (2008) Hybrid Barrier systems for Rockfall Protection Proceedings of the IDWRP, Switzerland.
- Gerber W.(2001) Guideline for the approval of rockfall protection kits, Swiss Federal Research Institute WSL Birmensdorf.
- Glover, J., A.Volkwein, F. Dufour, M. Denk & A. Roth (2010), Rockfall attenuator and hybrid drape systems - design and testing considerations, Proceedings of the AGS, Tunisia.
- Mikromak, (2008) WINalyze software, <http://www.winanalyze.com/index.htm>
- RAMMS (2010) http://www.wsl.ch/fe/lms/projekte/rapid_mass_movements/index_EN
- Rockyfor3D (2010) <http://www.ecorisq.org/docs/Rockyfor3D.pdf>